Chapter 5

Influence of Aromaticity on the Magneto Structural Property of Heteroverdazyl Diradicals

This chapter describes theoretical design of 5 different meta phenylene coupled high spin bis-heteroverdazyl diradicals and their analogous para phenylene coupled low spin positional isomers. The geometry based aromaticity index, harmonic oscillator model of aromaticity (HOMA) values for both the couplers (local HOMA) and the whole diradicals (global HOMA) have been calculated for all diradicals. We also qualitatively relate these HOMA values with the intramolecular magnetic exchange coupling constants (J) which is calculated using broken symmetry approach within unrestricted density functional theory framework. Structural aromaticity index HOMA of linkage specific benzene rings in our designed diradical systems shows that the aromatic character depends on the planarity of the molecule and it controls the sign and magnitude of J. The effect of the spin leakage phenomenon on J and HOMA values of certain phosphaverdazyl systems has been explicitly discussed. We also estimate another aromaticity index, nucleus independent chemical shift (NICS) values for the phenylene coupler in each diradical and compare these values with that of HOMA.

5.1. Introduction

The term aromaticity is primarily used in a chemical sense in early 19th century to portray a special class of organic substances.[1,2] However, it remains a mystery to the scientific community even today as there is no unique definition of aromaticity and it is multidimensional in nature. Nevertheless, the aromaticity can be characterized through the properties like (a) planarity (b) total $(4n+2)\pi$ electrons (c) stabilization energie,[3,4] (d) bond length,[5] (e) magnetic exaltation,[6] (f) retention of π–electron delocalization after typical reactions[7] and so on. If any system has all the characteristics mentioned above then it is fully aromatic. The lack of proper definition leads one to assign different indices to quantify aromaticity; these include different structural indices such as HOMA which can reliably give the differences in aromaticity in more complicated systems.[8] HOMA quantifies the decrease in aromaticity with an increase in the bond length alternation and bond elongation.[9] Aromaticity can not only be illustrated by geometry based indices, but also a specified π–electron part in some greater π–electron structure may be affected by its structural environment.[8–10] Beside structural HOMA index nucleus independent chemical shift (NICS) is another widely used index of aromaticity because of its simplicity and efficiency.[11-13] It is well known that, the extent of aromaticity can be established experimentally by the ^{1}H NMR shift of aromatic and anti-aromatic compounds. This effect is a manifestation of the π-electron ring current of aromatic systems under the influence of external magnetic field. NICS can be widely used to identify aromaticity, non-aromaticity and anti-aromaticity of a single ring system and individual ring in polycyclic systems (local aromaticity).

The design and synthesis of high spin magnetic molecules of organic origin have attracted wide attention during last three decades.[14,15] The magnetic properties of a crystalline material are known to be controlled by the intermolecular interaction which depends on the structure and the nature of the crystal. Similarly, for diradical based magnets, magnetic properties are dependent on the intramolecular magnetic exchange interaction which in turn depends on the structure and topology of the molecule.[14] Stable organic radicals in pure state are the most suitable precursor for diradical based magnets. More specifically, stable diradical species based organic ferromagnets are of primary interest in the study of molecular

magnetism.[16] The first reported species of the stable magnetically active radical was β-crystal phase of *p*-nitrophenyl nitronyl nitroxide.[17] After its discovery by Kinosita and co-workers in 1991 nitronyl nitroxide based diradicals with different couplers have been extensively investigated and characterized by many group of researchers.[18-20] There were many investigations to synthesize other radical species such as verdazyl, imino nitroxide, tetrathiafulvalene which are stable at high temperature and are suitable candidates for preparing organic diradical based ferromagnets,[21-25] at relatively higher temperature.

Verdazyl radical has a prolonged history of magnetism as it is very stable and fulfills almost all the necessary requirements for being used as stable diradical based magnets.[26-30] In general, verdazyl based diradicals are known to have the structure as shown in Scheme 5.1. In recent years, lots of effort is given to synthesize and characterize the "so-called" heteroverdazyl radicals incorporating different hetero atoms in place of nitrogen and carbon ring atoms at X or Y position or the both.[31] The most common heteroverdazyls are oxoverdazyls, thioverdazyls and phosphaverdazyls which are in general considered as the inorganic analogue of verdazyl radical.

Oxoverdazyls have C=O substitution at the Y position which interacts with the heterocyclic π-system through the π^* orbital of C=O and in turn gives the observed stability and planarity of the radical.[16] 1,3,5-triphenyl-verdazyl and 1,3,5-triphenyl-oxoverdazyl radicals have been isolated and characterized.[32] It has been found that bis-oxoverdazyl diradical has singlet ground state. However, insertion of suitable coupler between the two radical centers results in the formation of diradical with triplet ground state.

Substitution of the oxygen atom of oxoverdazyl moiety with less electronegative sulfur atom gives thioverdazyl radical moiety with a notable variation of electron density from its oxo-analogue. Like other verdazyl derivatives, suitable choice of coupler gives stable thioverdazyl diradical with triplet ground state.[32,33]

In the case of phosphaverdazyls, one of the skeleton carbon atoms of verdazyl radical is replaced by phosphorus atom. There are two positions in verdazyl radical where carbon atom can be replaced by phosphorus atom. Hence, the two structurally different

phosphaverdazyls have been reported.[16] *Firstly*, the C=O group can be replaced by P=O group resulting a non planar phosphaverdazyl. *Secondly*, the carbon atom at the X position is replaced by P atom (Scheme 5.1). The second one has σ- and π-systems which mix with each other leading to the spin leakage from the P-atom.[31] Due to spin leakage the spin density of a particular atom at a particular site becomes lower than the expected spin density value of that particular site. The spin leakage has a profound effect on magnetic behavior of the concerned diradical. This phenomenon will be discussed later in this article. A number of different phosphaverdazyl radicals have been prepared and characterized by Hicks and co-workers. These radicals show characteristic EPR signal. Moreover, the hyperfine parameters of these systems and that of oxoverdazyl radicals are almost similar.[31] They have established that the method of synthesis of phosphaverdazyls is theoretically analogous with that of oxo- and thio-verdazyls.[32]

Scheme 5.1. Schematic diagrams of benzene coupled bis-heteroverdazyl systems, where the spacer is *meta* phenylene ring (S1) for Set-a diradicals (1a, 2a, 3a, 4a and 5a respectively) and *para* phenylene ring (S2) for Set-b diradicals (1b, 2b, 3b, 4b and 5b respectively). Substitution at 'X' and 'Y' positions gives rise to different "so-called" bis-heteroverdazyl diradical species. Here $\varphi_1$and φ_2 denotes the dihedral angle between the plane of spacer and that of the verdazyl radicals.

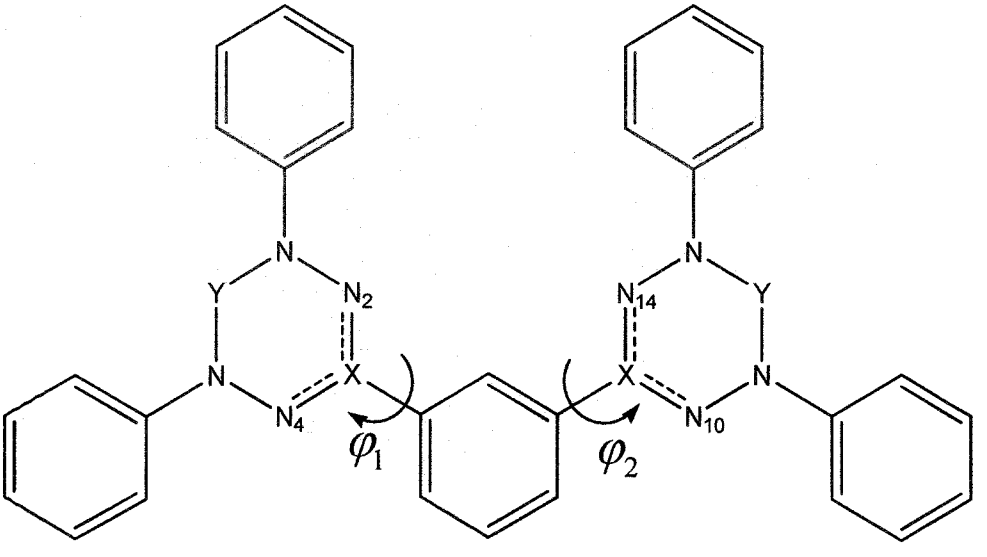

(S1)

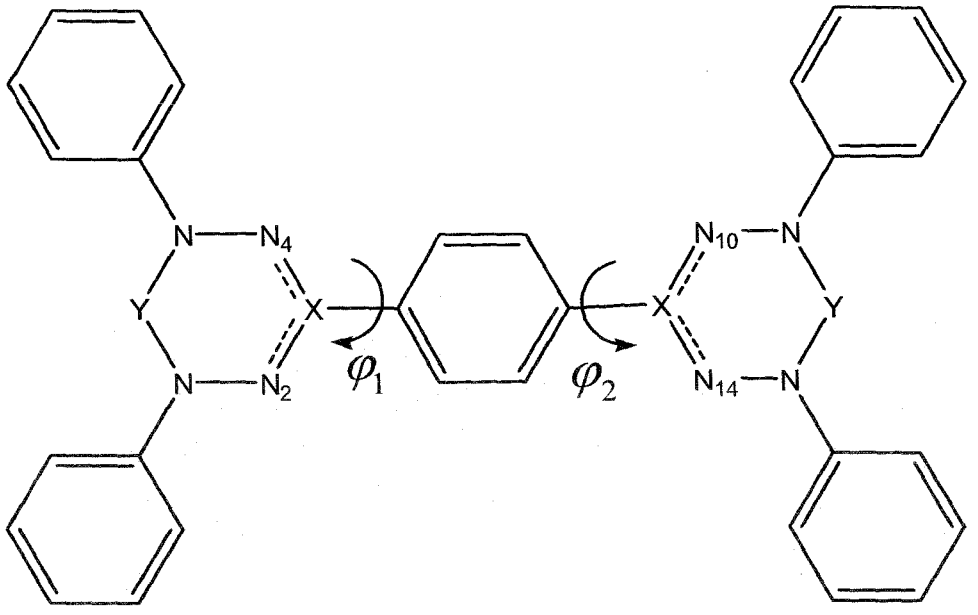

(S2)

In the present chapter, we design and theoretically characterize *meta*-phenylene coupled [Set-a denoted as 1(a), 2(a), 3(a), 4(a), 5(a)) and *para*-phenylene coupled (Set-b denoted as 1(b), 2(b), 3(b), 4(b), 5(b)] diradicals with verdazyl, oxoverdazyl, phosphaverdazyl and thioverdazyl radical centers (Figure 5.1 and also see Scheme 5.2). We design this type of heteroverdazyls based on the fact that very similar types of N-phenyl substituted verdazyl radicals, like 2,4,6-triphenylverdazyl radicals, have already been synthesized and characterized.[34-37] As far as the synthesis of these diradicals is concerned, the synthetic routes of verdazyl radicals with a range of substituents on the nitrogen and carbon atoms are well known. These radicals are air and moisture sustainable and can be easily handled in laboratory. However, magnetic properties of these diradicals have been determined by semi empirical methods.[31] Our primary aim of this chapter is to theoretically investigate the effect of aromaticity of the couplers and that of the molecules as a whole on the magnetic exchange between two monoradical moieties. We report the popular geometry based aromaticity index, Harmonic Oscillator Model of Aromaticity (HOMA)[9,38,39] individually for the couplers and the whole diradicals. We also calculate NICS values for the phenylene coupler in each diradical and compare them with HOMA. A qualitative correlation between the energy differences of two singly occupied molecular orbitals (SOMOs) with the J values has been given.

5.2. Theoretical Background and Methodology

The structural data for calculation of HOMA values of all the diradicals under discussion is taken from the optimized geometries of the diradicals. In this chapter, the molecular geometries of all the molecules (Set-a and Set-b) have been fully optimized with the UB3LYP[40,41] exchange correlation potential using 6-31G(d,p)[42-44] basis set. The optimized geometries are shown in Figure 5.1. The Harmonic Oscillator Model of Aromaticity (HOMA) is an easily accessible geometry based quantitative index of total aromaticity and is defined using the degree of bond length alteration. The advantage of HOMA over other energy based aromaticity index is due to the possibility of using HOMA either for the whole molecule (global HOMA) or for any fragment of the molecule (local HOMA) having π-electron networks. Nonetheless, it can not be limited only for the hydroca-

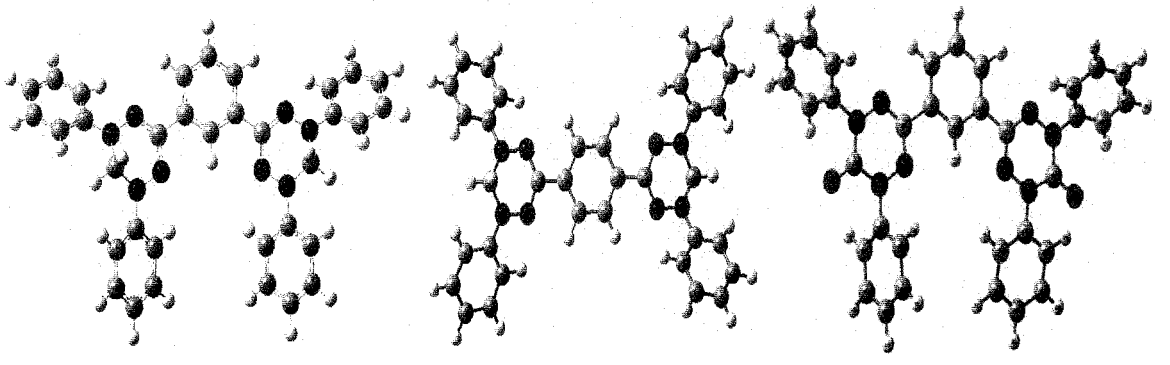

(1a) **(1b)** **2(a)**

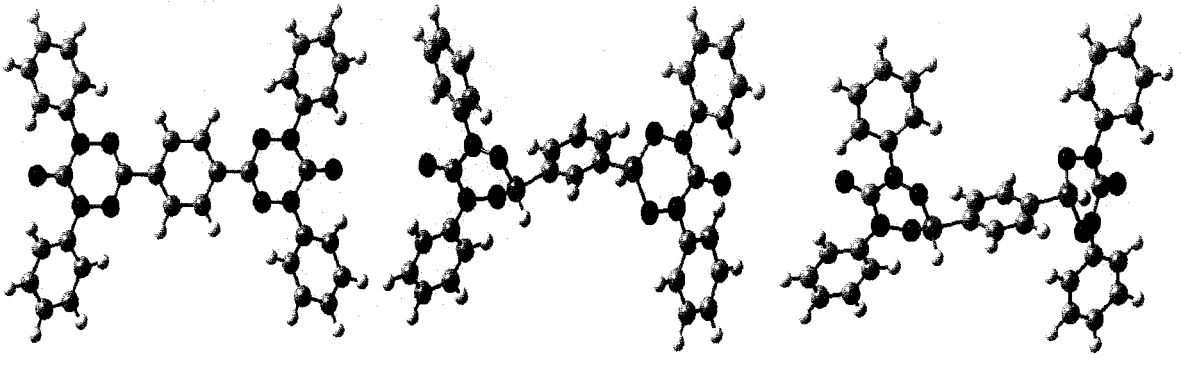

2(b) **(3a)** **(3b)**

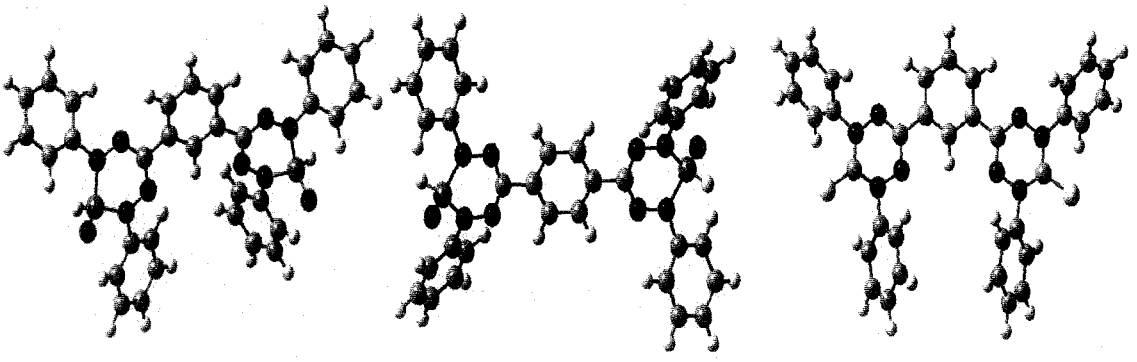

(4a) (4b) (5a)

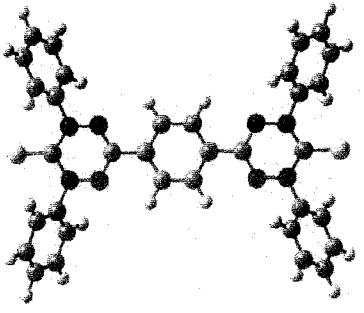

(5b)

Figure 5.1. The optimized geometries of different bis-heteroverdazyl diradical systems with m-phenylene coupler (Set-a: 1a, 2a, 3a, 4a and 5a) and with p-phenylene coupler (Set-b: 1b, 2b, 3b, 4b and 5b) from UB3LYP calculations with the 6-31G(d,p) basis set. The carbon atoms are marked in grey, sulfur in yellow, nitrogen in blue, oxygen in red, phosphorus in orange, and hydrogen in white respectively.

-rbon system. We choose HOMA aromaticity index because of its easy calculation and wide application.[38,39] The HOMA of a species can be calculated as,

$$\text{HOMA} = 1 - \alpha/n \sum (R_{opt} - R_{ij})^2, \quad (5.1)$$

where n is the number of bonds taken into summation, R_{opt} is the optimal bond for fully delocalized π–electron system, R_{ij} is the bond length of the molecule under investigation. HOMA is also a normalized index of aromaticity. It is known that HOMA value closer to the ideal value of 1 indicates the presence of greater aromaticity, whereas, HOMA value equal to

zero indicates non-aromatic system. The parameter α is an empirical constant set to give HOMA to be 0 and 1 for fully non-aromatic and fully aromatic systems respectively. It can also be noted here that, HOMA of bare benzene is 0.969, 0.979 and 0.996 from electron diffraction geometry, from MW (microwave) geometry and from X-ray geometry respectively.[38] In the present chapter, we have determined the HOMA values individually for the couplers and the whole diradicals, the details of which is given in results and discussion section.

In another way, the aromaticity of the couplers has been estimated by NICS index using UB3LYP/GIAO methodology with 6-31G(d,p) basis set for the phenylene coupler in each diradical. The NICS values can be calculated at the centre of the rings [NICS(0)]. The σ framework of C-C and C-H affects the π-electrons and hence NICS is calculated at 1Å above the ring surface [NICS(1)] where the π-electron density is known to be maximum.[11-13]

Using optimized geometries we also calculate the energies of different spin states of the diradical required for estimation of magnetic exchange coupling constant. The magnetic exchange interaction energy between two magnetic sites 1 and 2 is given by the well known Heisenberg-Dirac-van Vleck (HDvV) spin Hamiltonian

$$\hat{H} = -2J\hat{S}_1 \bullet \hat{S}_2, \tag{5.2}$$

where, J is the exchange coupling constant between two magnetic centers, $\hat{S}_i$ is the spin angular momentum operator of ith site. In case of ferromagnetic interaction between two parallel spins, J value is positive, whereas the negative J indicates an antiferromagnetic interaction between two antiparallel spins. The quantity J can be estimated from the energy difference of high spin and low spin states of the magnetically active molecule. As an example, J value of a diradical with single unpaired electron on each site can be written as

$$E_{(S=1)} - E_{(S=0)} = -2J. \tag{5.3}$$

However, pure singlet state of a diradical can not be truly represented by a single determinant (SD) wave function in the unrestricted formalism and this leads to spin contamination in such calculations. One may make use of multiconfigurational methods to describe pure spin states in an appropriate way. However, those methods are computationally expensive and generally not used for large systems. An alternative way is the Broken Symmetry (BS) formalism proposed by Noodleman in DFT framework.[45,46] The BS state is an equal mixture of a singlet and a triplet state and is not an eigenstate of the above Hamiltonian (eq 5.2). Nevertheless, the BS state is a spin contaminated state and one needs spin projection technique for reliable estimation of the magnetic exchange coupling constant. Depending upon the extent of overlap between the magnetic orbitals, J can be estimated in number of ways,[47-62] using unrestricted spin polarized BS solution for lower spin state. However, it has been established[19,20,34,60-64] unambiguously that the following formula by Yamaguchi and co-workers, is the most appropriate one for estimating magnetic exchange coupling constant of diradicals of organic origin. The formula is written as

$$J = \frac{(E_{BS} - E_T)}{\langle S^2 \rangle_T - \langle S^2 \rangle_{BS}}, \tag{5.4}$$

where E_{BS} and E_T denotes the energy of the broken symmetry state and triplet state respectively. The quantities $\langle S^2 \rangle_{BS}$ and $\langle S^2 \rangle_T$ represent square of the total spin for BS and triplet state respectively.

It is well known that commonly used DFT exchange correlation potentials overestimates J values due to the presence of high self interaction error (SIE). To avoid SIE problem, hybrid functionals such as B3LYP are used in BS-UDFT calculations, especially for spin projected techniques that are used to evaluate J.[65,66] Based on these molecular geometries the corresponding J values of each molecule have been estimated from the single point energies of the triplet and BS states. These single point calculations are carried out using UB3LYP method with 6-311++G(d,p) basis set. To obtain open shell BS singlet solution "guess =mix" keyword is used within unrestricted formalism. The BS states for all diradicals are stable. All the calculations have been carried out using GAUSSIAN 03W[67]

quantum chemical package. We also have used Hyperchem 7.5[68] and Molekel 4.0[69] for visualization.

5.3. Results and Discussion

In general, aromaticity depends on the topology of the molecules. Above all, a planar structure favors aromaticity. Here, we observe that the optimized structures of all the heteroverdazyl diradicals are nonplanar. This non planarity of the heteroverdazyls affects the aromaticity as well as the magnetic behavior of the diradical. In determining the sign and magnitude of J of the diradical the geometry of the spacer between two verdazyl moieties is the key factor.

In this present study, the HOMA values are calculated from the data of optimized structures. We have calculated the hitherto undetermined optimal bond lengths (R_{opt}) and the empirical constants α for PO and PN bonds using the experimentally determined single and double bond lengths of the PO and PN bonds. For this purpose we have used eq (6), (7), and (8) of ref. 38. These values are reported in Table 5.1. The experimental data for single and double bond lengths of PO and PN bonds are taken from the work of Hoppe et al.[70] and Markovski et al.[71] respectively.

Table 5.1. Reference single and double bond lengths and approximate optimal bond length, and empirical constant α.

Type of bond	$R_s^{\#}$	R_d^{*}	R_{opt}	α
PO	1.581[a]	1.432[a]	1.482	162.59
PN	1.770[b]	1.530[b]	1.610	62.5

[#]Single bond distance, *Double bond distance, [a]Data from ref. [70], [b]Values from ref. [71].

It has been observed that the HOMA values for phenylene couplers are higher in *meta*-connected diradicals than that in corresponding *para*-connected species (Table 5.2). This is probably due to the fact that π-electron delocalization is lower in *para*-connected diradicals than that of consequent *meta*-connected one. Therefore, one can easily infer that *meta*-connected couplers (Set-a) are more aromatic than the corresponding *para*-connected couplers (Set-b), that is, the delocalization of π–electrons is better among the *meta*-coupler moiety, which favors ferromagnetic interaction between the radical centers attached to the coupler due to itinerant exchange, hence, aromaticity favors the ferromagnetic trend.[19,64]

Table 5.2. Variation of HOMA values for couplers and for the whole diradicals at UB3LYP level of theory with 6-31G(d,p) basis set. Here $\varphi_1$and φ_2 are the dihedral angles (Scheme 5.1) between the two heteroverdazyl moieties with the plane of the coupler.

Set	Diradicals	HOMA for coupler	HOMA for the whole diradical	Dihedral Angle (deg)		
				φ_1	φ_2	Average
Set-a	(1a)	0.96488	0.71024	3.0604	3.0415	3.0510
	(2a)	0.96863	0.72301	6.2164	9.1013	7.6589
	(3a)	0.96822	0.66664	86.1027	86.2033	86.1530
	(4a)	0.96845	0.71712	9.5952	10.0079	9.8016
	(5a)	0.96515	0.74477	–0.3489	0.3824	0.0168
Set-b	(1b)	0.95898	0.70706	2.4790	2.4776	2.4783
	(2b)	0.96209	0.72536	0.5116	0.5116	0.5116
	(3b)	0.96520	0.65616	85.1074	85.1075	85.1075
	(4b)	0.96246	0.73659	0.8646	0.8633	0.8640
	(5b)	0.95807	0.74744	0.7353	0.7354	0.7354

It is established that the unpaired spins of verdazyls are equally distributed among magnetic centers comprising of the specified atoms (N_2, N_4, N_{10} and N_{14}, Scheme 5.1) of the diradicals[32] except the diradicals with phosphaverdazyl radical centers which shows the spin leakage from the phosphorous atom. In case of phosphaverdazyl diradicals, the spin distribution over the specific magnetic centers is unequal. This results in the low J value of the diradical.[24,31] The J values are calculated using eq (5.4). We observe that the more aromatic *meta*-connected molecules (Set-a) are ferromagnetically coupled while the less aromatic *para*-connected molecules (Set-b) are antiferromagnetically coupled. The calculated J values are reported in Table 5.3. These observations follow same trend as found in previous work with different diradicals.[19,20,33,64] A discussion on the magnetic properties of molecule 1(a) and 1(b) is due here. One can easily notice that the molecule (1a) is ferromagnetic whereas the molecule (1b) is antiferromagnetic, which strongly contradicts with the reports claiming that both the molecules possess triplet ground state with exchange energies in excess of 300K.[32,35-37] However, a relatively new experimental study on benzene bridged diradicals of very similar structure reveals that the *para*-connected diradical is antiferromagnetic whereas the *meta*-connected is ferromagnetic one. Our calculation is in good agreement with the later observation. This problem was addressed previously in a review by Koivisto and Hicks lacking a proper theoretical explanation.[32] We unequivocally settle this problem here.

The change in HOMA values with dihedral angle between the spacer plane and that of the radical moieties (Table 5.2) of the whole diradical molecule shows that aromaticity is highly disturbed in (3a) due to high average dihedral angle. This results in the lowest magnetic exchange coupling constant J = 02 cm^{-1} in diradical (3a). It is also evident that diradical (5a) have highest HOMA value with maximum J = 42 cm^{-1} (Table 5.3) among the ferromagnetic series for having low average dihedral angle between the coupler plane and the plane of the radical moieties. In case of diradical (1a) and (2a), as the global HOMA increases the J value also increases. Among the Set-b diradicals low global HOMA is observed for diradical (3b) with very high average dihedral angle. In any case, for all 10 different bis-heteroverdazyl diradicals, the HOMA values are smaller for the benzene acting as a linkage specific coupler between the two radical moieties (Table 5.2) than the HOMA value obtained for bare benzene i.e. $(HOMA)_{\text{coupler benzene}} < (HOMA)_{\text{bare benzene}}$ is observed.

Table 5.3. Calculated absolute energies in atomic unit (*au*), the $\langle S^2 \rangle$ value and intramolecular magnetic exchange coupling constant (J in cm^{-1}) using UB3LYP/6-31G(d,p) and 6-311++G(d,p) for different *meta*-connected (Set-a) and *para*-connected bis-heteroverdazyl diradicals (Set-b).

	At UB3LYP/6-31G(d,p) level			At UB3LYP/6-311++G(d,p) level		
Diradicals	E_{BS} (au)	E_T (au)	J(cm^{-1})	E_{BS} (au)	E_T (au)	J(cm^{-1})
	$\langle S^2 \rangle$	$\langle S^2 \rangle$		$\langle S^2 \rangle$	$\langle S^2 \rangle$	
(1a)	–1750.44633	–1750.44659	57	–1750.78001	–1750.78017	35
	1.049	2.050		1.045	2.047	
(2a)	–1898.47016	–1898.47023	15	–1898.90690	–1898.90708	39
	1.043	2.049		1.042	2.047	
(3a)	–2506.04818	–2506.04834	35	–2506.52823	–2506.52824	02
	1.014	2.014		1.014	2.014	
(4a)	–2506.17215	–2506.17216	02	–2506.64695	–2506.64714	41
	1.046	2.054		1.046	2.051	
(5a)	–2544.35946	–2544.35978	70	–2544.80009	–2544.80028	42
	1.043	2.049		1.043	2.047	
(1b)	–1750.39137	–1750.39105	–71	–1750.44770	–1750.44731	–87
	1.058	2.046		1.055	2.040	
(2b)	–1898.47136	–1898.47084	–115	–1898.90810	–1898.90776	–76
	1.053	2.042		1.051	2.039	
(3b)	–2506.04410	–2506.04405	–11	–2506.52368	–2506.52365	–07
	1.013	2.014		1.013	2.014	
(4b)	–2506.17349	–2506.17324	–55	–2506.64848	–2506.64814	–75
	1.057	2.046		1.055	2.044	
(5b)	–2544.36077	–2544.36063	–31	–2544.41592	–2544.41563	–64
	1.050	2.042		1.051	2.041	

A precise definition of aromaticity is not possible due to its multidimensional nature; hence there is no exact scale to measure it. Therefore, we have also calculated another aromaticity index NICS to comprehend the aromatic character of all the diradicals. Here, NICS(0) and NICS(1) values have been calculated for the phenylene coupler in all 10 bis-heteroverdazyl diradicals. Probes (dummy atoms) are placed at the centre of the ring to compute NICS(0) values and 1Å above the ring surface where π-orbital density is maximum to get NICS(1) values.[11-13] These values are reported in Table 5.4. Here, we also estimate NICS(0) and NICS(1) values for the bare benzene ring at same level of theory. These values are –9.82 and –11.32 respectively. Comparing these NICS values of bare benzene with that of the coupler benzene (Table 5.4), one can very easily surmise that $(NICS)_{coupler\ benzene}$ is less than $(NICS)_{bare\ benzene}$. This is also evident from HOMA values reported in Table 5.2. It is also to be concluded from Table 5.4 that, in every case NICS [NICS(0) and/or NICS(1)] values for the couplers of *meta*-phenylene coupled Set-a diradicals are more negative than their Set-b counterparts, that is, couplers of Set-a diradicals are more aromatic than their corresponding Set-b diradicals. These results are also in good agreement with the HOMA values (Table 5.2), that means HOMA correlates well with NICS.[9,10] From these results one can also conclude that as the couplers of the Set-a diradicals are more aromatic than corresponding Set-b diradicals aromaticity of the coupler favors the ferromagnetic trend which has already been established from the HOMA analysis.

Table 5.4. The calculated NICS(0) and NICS(1) values for the all the ten diradicals at UB3LYP level of theory using 6-31G(d,p) basis set.

Diradicals	NICS(0)	NICS(1)	Diradicals	NICS(0)	NICS(1)
1(a)	−7.60	−9.72	1(a)	−7.59	−9.59
2(a)	−7.90	−9.91	2(a)	−7.89	−9.84
3(a)	−8.54	−11.21	3(a)	−8.42	−11.18
4(a)	−7.87	−9.88	4(a)	−7.86	−9.76
5(a)	−7.98	−10.04	5(a)	−7.95	−10.00

Here we focus on the spin leakage of phosphaverdazyls. As mentioned earlier, Hicks and co-workers[31,32] have shown that due to spin leakage, density of electron spin on linkage phosphorus atom in (3a) and (3b) diradicals decreases in comparison with the spin density found on the linkage carbon atom at the same position of corresponding oxoverdazyls (2a) and (2b). A detail analysis of Mulliken spin densities of (2a) and (3a) diradicals shows a comparatively lower spin density over the P atom (–0.004048) of the phosphaverdazyl (3a) than that over the C atom of corresponding oxoverdazyl (–0.144519) (2a). At the same time, it is found that nitrogen atoms (N_2, N_4, N_{10} and N_{14} in Scheme 5.1) adjacent to P atom at position X in (3a) and (3b) bears more electron spin density than the corresponding nitrogen atoms (N_2, N_4, N_{10} and N_{14} in Scheme 5.1) adjacent to the carbon atom in X position in (2a) and (2b). In case of (3a) and (3b), the electron spin density is about 0.50703 on the nitrogen atoms N_2, N_4, N_{10} and N_{14} (Scheme 5.1) while on the corresponding nitrogen atoms in molecules (2a) and (2b), the electron spin density is about 0.37912. The overall average spin density on N atoms (N_2, N_4, N_{10} and N_{14}) is lower in case of (3a) and (3b) diradicals than that in case of (2a) and (2b) diradicals respectively. We notice that this spin delocalization effect is more clearly observable if one carries out simulations using diffused basis set. Incase of diradical (3a), we get a lower value of J from the calculations carried out using more diffused basis set 6-311++G(d,p) than that obtained from the calculations carried out using 6-31G(d,p) basis set. For the same reason, in case of (3b) the J value obtained from the calculations using 6-311++G(d,p) is higher than that obtained from the calculations using 6-31G(d,p) basis.

So far a quantitative estimation of aromaticity of the diradicals and its effect on magnetic exchange has been discussed. However, we reach at a very similar qualitative conclusion about the state of magnetism of the diradicals using spin alternation rule, which is essentially based on Hund's rule[72,74] The presence of even number of bonds between the two magnetic centers gives rise to ferromagnetic interactions but antiferromagnetism arises in case of odd number of bonds.[19,20] The existence of apparently two different spin polarization paths, presence of heteroatom in the spinning path and non planarity of the system makes the prediction of magnetic characteristics of molecular systems a tricky job.[74] However, Ali and Datta have explicitly shown that

using spin alternation rule qualitative prediction of magnetic characteristics of any diradical system can be given satisfactorily,[19,20] provided one takes into account of the fact that nitrogen, oxygen, sulfur like heteroatom may contribute two π-electrons depending on the bonding pattern, nature and topology of the coupler moiety.[19] In our present chapter, we explicitly show that according to the spin alternation rule molecules of Set-a, which are essentially *m*-phenylene coupled diradicals, give ferromagnetic interaction with positive J value and those of Set-b, that is *p*-phenylene coupled diradicals (Scheme 5.2), shows antiferromagnetic interaction with negative J value. The same can also be established by spin density plots (Figure 5.2). This estimation is supported by the results of our calculations as discussed earlier.

Scheme 5.2. Schematic representation of the ground spin states and the nature of the magnetic exchange coupling on the basis of spin alternation rule for different linkage specific phenylene bridged bis-heteroverdazyl diradicals.

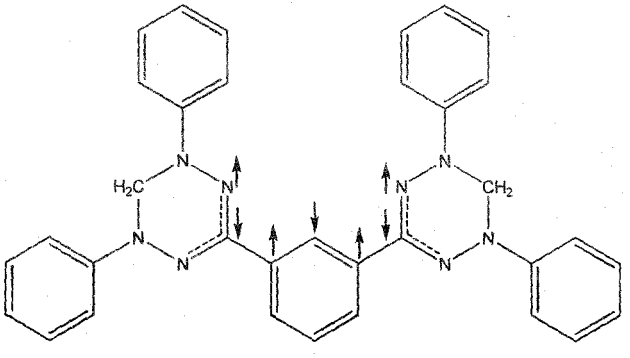

(1a)

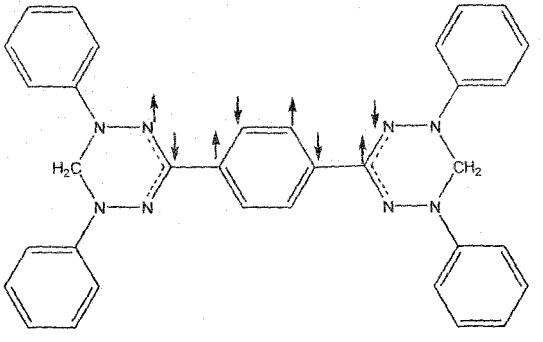

(1b)

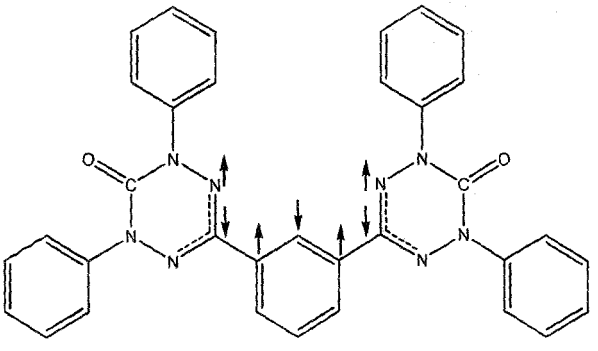

(2a)

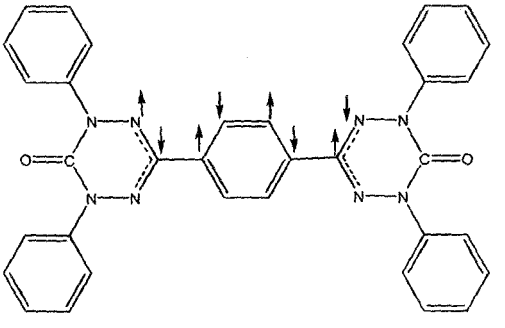

(2b)

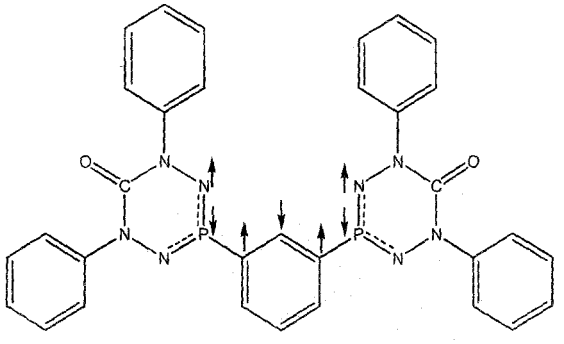

(3a)

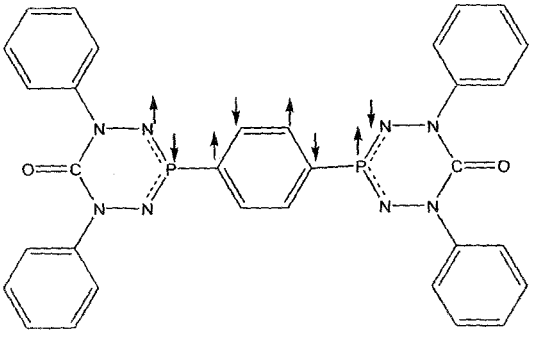

(3b)

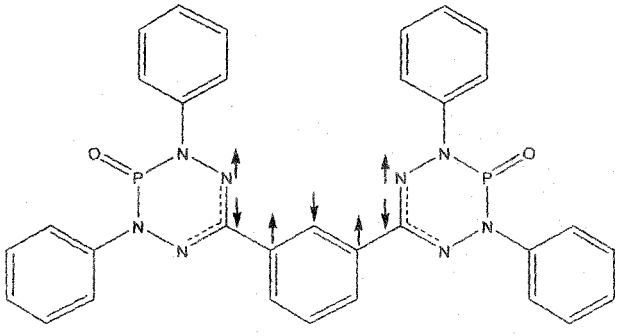

(4a)

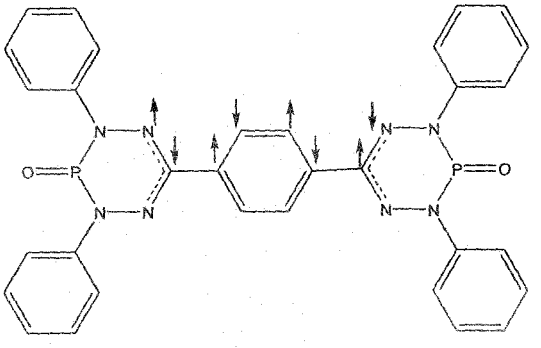

(4b)

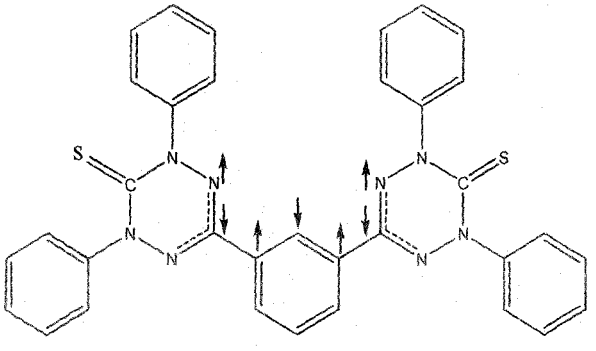

(5a)

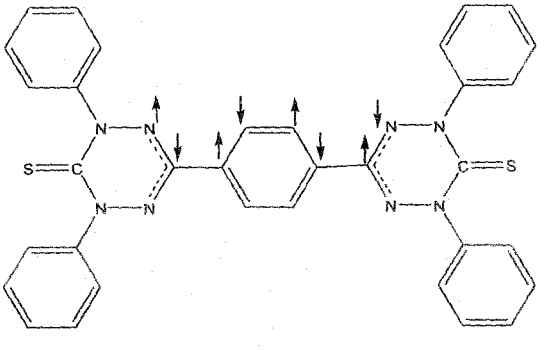

(5b)

On the basis of all valence electron independent particle model on benzyne and diradicals Hoffmann et al. have suggested that if the energy difference between two consecutive SOMOs is less than 1.5 *eV* parallel orientation of spins occur.[75] In another study, Constantinides et al.[76] have showed that for $4n\pi$ antiaromatic linear and angular polyheteroacenes ΔE_{SS} value will be greater than 1.3 *eV*, resulting in antiparallel orientation of spins. Using DFT calculations, however, Zhang et al.[77] have shown that the

magnetic characteristics of a molecule are not explicitly dependent on the critical value of ΔE_{SS} rather it is different in different cases. We find that for the ferromagnetic diradical series (Set-a) the calculated J values decreases as the ΔE_{SS} values increases, where both of the quantities (J and ΔE_{SS}) have been calculated using 6-31G(d,p) basis set at the

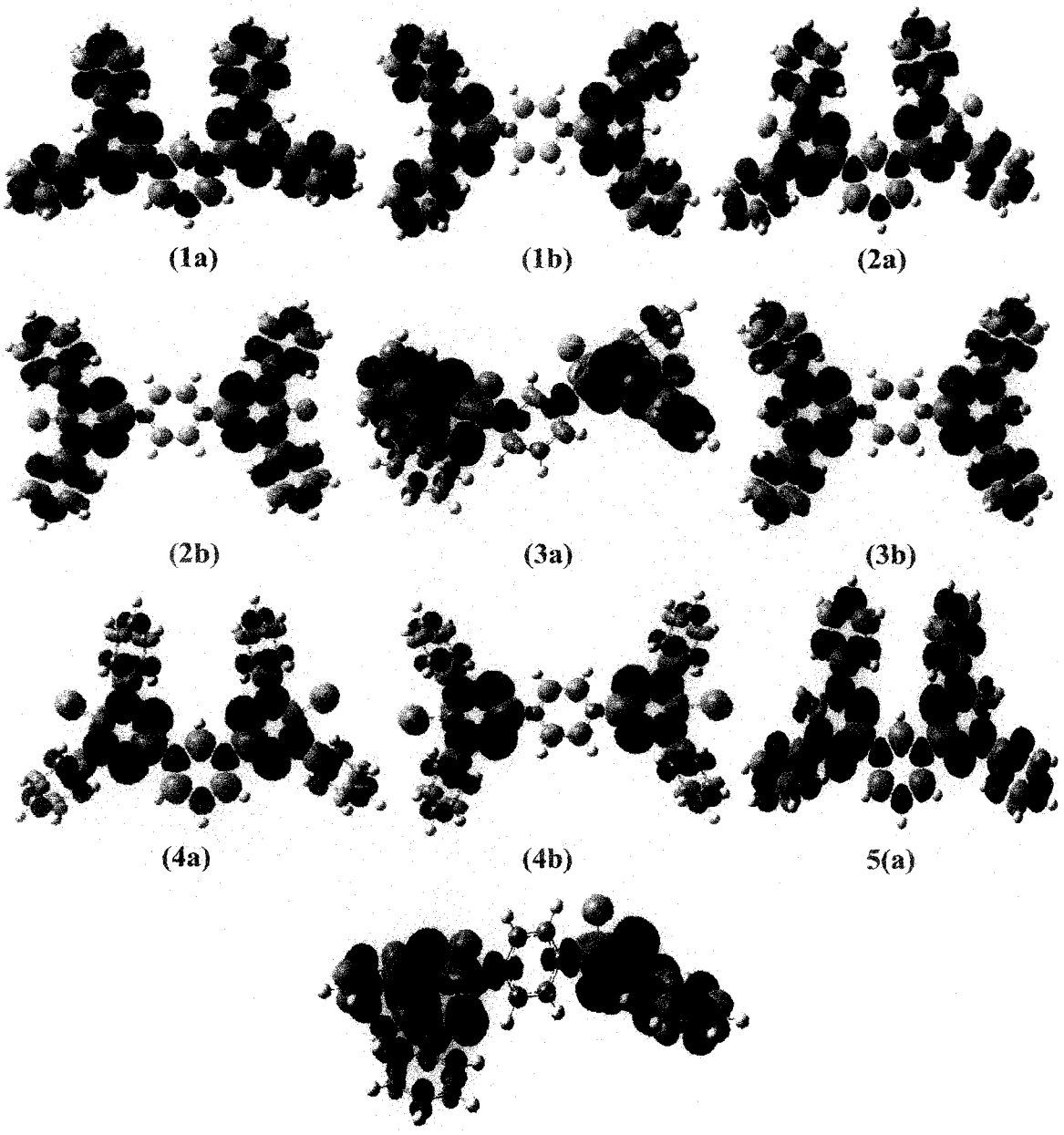

Figure 5.2. Spin density plots for different phenylene bridged bis-heteroverdazyl diradicals (Set-a and Set-b). Purple color indicates α–spin and green color indicates β–spin respectively. The cut off values for this all 10 figures were 0.0004.

UB3LYP level of theory. The highest J value is obtained for diradical (5a) with the lowest value of ΔE_{SS}. On the other hand, the lowest J with highest ΔE_{SS} is obtained in case of diradical (4a). In case of diradical (2a), (3a), and (4a), as ΔE_{SS} value decreases down the series the J value increases (Table 5.5). These observations prove that our calculations agree with the Hay-Thibeault-Hoffmann (HTH) formula[78] for the singlet–triplet energy gap in weakly coupled binuclear metal complexes. This observation is also in accordance with other previous theoretical work.[19,20,34,63,64]

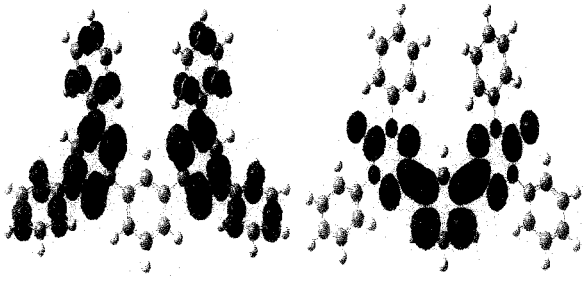

1(a) [Disjoint]

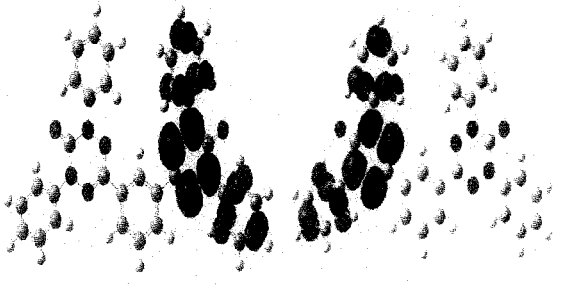

2(a) [Disjoint]

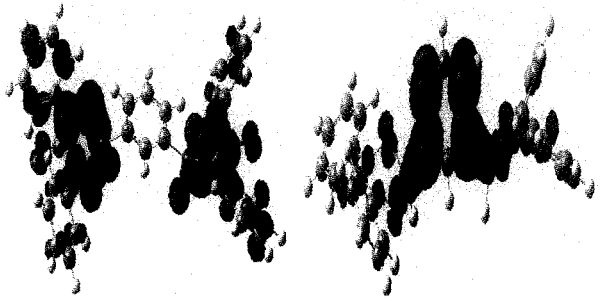

3(a) [Disjoint]

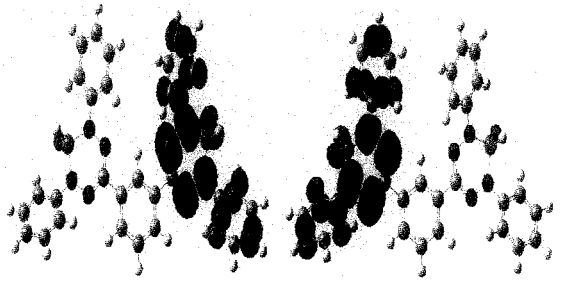

4(a) [Disjoint]

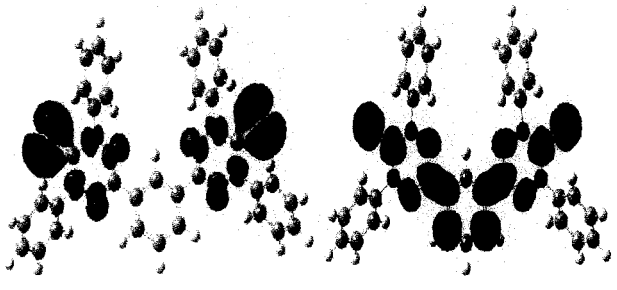

5(a) [Disjoint]

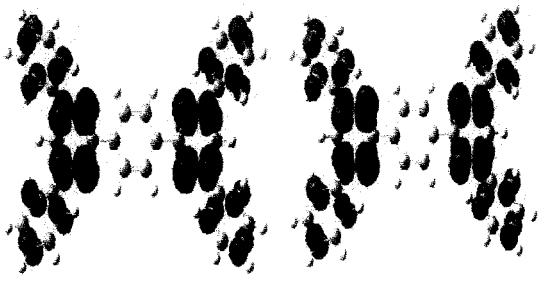

1(b) [Nondisjoint]

2(b) [Nondisjoint] **3(b) [Nondisjoint]**

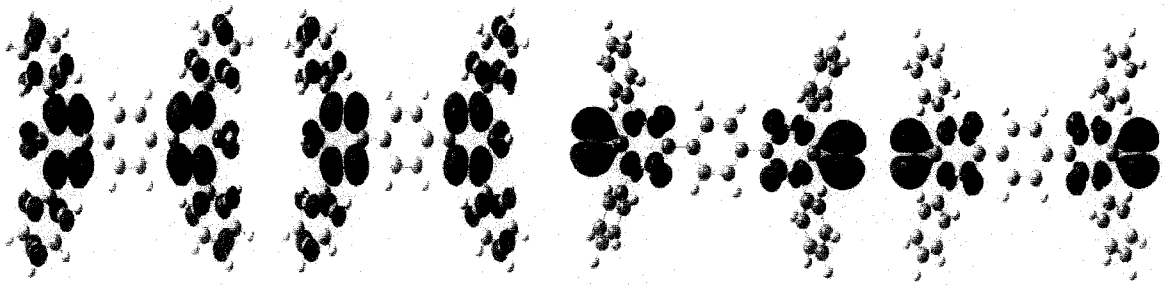

4(b) [Nondisjoint] **5(b) [Nondisjoint]**

Figure 5.3. The triplet disjoint and triplet nondisjoint sets of SOMOs for Set-a [1(a), 2(a), 3(a), 4(a) and 5(a)] and set-b [1(b), 2(b), 3(b), 4(b) and 5(b)] bis-heteroverdazyl diradicals. The diagrams are generated from the results of the calculation carried out using UB3LYP level of theory and 6-31G(d,p) basis set. The cut off values for this all 10 figures were 0.0004.

The shapes of the SOMOs (Figure 5.3) play a major role in determining the magnetic properties of the diradicals. We find that the SOMOs are disjoint (atoms are not common) for Set-a diradicals and nondisjoint (atoms are common) for Set-b diradicals. As a consequence, the diradicals of Set-a are ferromagnetic and that of Set-b are antiferromagnetic. These observations are also in tune with the previous studies[19,64] as well as with our present numerical calculations.

We investigate the energy difference between the highest occupied molecular orbital (HOMO) and lowest unoccupied molecular orbital (LUMO) energy gap of all the 10 molecules (Table 5.6). The HOMO–LUMO energy gap determines the fate of

numerous chemical reactions.[79] Consequently HOMO–LUMO energy gap is used as a simple indicator of kinetic stability. If the energy gap is high, it signifies high kinetic stability as well as low chemical reactivity and hence more aromatic.[80] The energy gap also corresponds to the chemical hardness of the molecule.[81] From Table 5.6, it is evident

Table 5.5. Absolute energies of SOMOs in atomic unit (*au*) and their differences in electron volt (*eV*) along with the *J* values (in cm^{-1}) for different bis-heteroverdazyl diradicals (Set-a and Set-b). All calculations are done using UB3LYP level of theory with 6-31G(d,p) basis set.

Diradicals	$E_S(1)$ *au*	$E_S(2)$ *au*	ΔE_{SS} in *eV*	$J(cm^{-1})$
(1a)	–0.16661	–0.16658	0.00082	57
(2a)	–0.19242	–0.19133	0.02966	15
(3a)	–0.20213	–0.20170	0.01170	35
(4a)	–0.18867	–0.18715	0.04136	02
(5a)	–0.19915	–0.19913	0.00054	70
(1b)	–0.16729	–0.16660	0.01878	–71
(2b)	–0.19262	–0.19161	0.02748	–115
(3b)	–0.20117	–0.20030	0.02367	–11
(4b)	–0.18814	–0.18715	0.02694	–55
(5b)	–0.20003	–0.19891	0.03048	–31

that all the Set-a diradicals have higher HOMO–LUMO energy gap than the corresponding antiferromagnetic Set-b series, which implies that the ferromagnetic Set-a diradicals are kinetically more stable, that is, chemically less reactive and more aromatic in comparison with the corresponding Set-b diradicals. It is also known that the molecules having HOMO–LUMO energy gap of the order of 1.59-3.18 *eV* can be suitable candidates for optoelectronic devices.[82] In that respect, more judicious designing of molecules may come up with good candidates for such applications. We hope to report such molecules in near future.

Table 5.6. The HOMO and LUMO energies in atomic unit (*au*) and their difference in electron volt (*eV*) for different bis-heteroverdazyl diradicals at UB3LYP level of theory with 6-31G(d,p) basis set.

Set	Diradicals	E_{HOMO} in *au*	E_{LUMO} in *au*	$\Delta E_{H\text{-}L}$ in *eV*
Set-a	(1a)	–0.16658	–0.02665	3.80772
	(2a)	–0.19133	–0.05166	3.80064
	(3a)	–0.20170	–0.06673	3.67275
	(4a)	–0.18715	–0.03821	4.05290
	(5a)	–0.19913	–0.06728	3.58785
Set-b	(1b)	–0.16660	–0.03767	3.50839
	(2b)	–0.19161	–0.06389	3.47547
	(3b)	–0.20030	–0.07653	3.36798
	(4b)	–0.18715	–0.05006	3.73044
	(5b)	–0.19891	–0.07854	3.27546

Table 5.7. Ground state energies of heteroverdazyl diradicals determined from the results of single point UB3LYP/6-311++G(d,p) calculations.

Set-a	E_T in *au*	Set-b	Estimated E_s in *au*
(1a)	–1750.78017	(1b)	–1750.44810
(2a)	–1898.90708	(2b)	–1898.90841
(3a)	–2506.52824	(3b)	–2506.52371
(4a)	–2506.64714	(4b)	–2506.64882
(5a)	–2544.80028	(5b)	–2544.41621

We have compared the ground state stability of the two different types of diradicals (Table 5.7). In general, ferromagnetic diradicals show grater stability than their antiferromagnetic counterparts. However, a little bit of over estimation of the energy value of the singlet state (E_S) is observed in two cases. Nonetheless, the estimated E_S values for Set-b diradicals are lower than the respective computed triplet state energy values (E_T), that is, singlet ground states for Set-b diradicals are confirmed.

5.4. Conclusions

This chapter presents a theoretical study of correlation between structural aromaticity index HOMA and intramolecular magnetic exchange coupling in *m*-phenylene and *p*-phenylene coupled bis-heteroverdazyl diradicals. The HOMA index which depends on the structure of the molecules is estimated for the whole diradical molecules and their aromatic coupler fragments to show how intramolecular magnetic interaction is dependent on the aromatic character of the diradical. The HOMA values suggest that increase of aromaticity is associated with the enhancement of ferromagnetism, that is, aromaticity favors ferromagnetic trend in such systems. It can be observed that low HOMA value is observed in case of diradical (3a) and (3b), where spin leakage is prominent. Resembling structural aromaticity index HOMA, the magnetic aromaticity index nucleus independent chemical shift (NICS) also shows that the ferromagnetism is instigated by the aromaticity of the coupler of the diradicals.

In this chapter we find, Set-a diradicals are ferromagnetic where as Set-b diradicals are antiferromagnetic in nature. The exchange-coupling interactions are mainly transmitted through conjugated π-electron system as observed and justified by other authors.[19,20,34,41,42,44] We also show that the low J values for bis-phosphaverdazyl diradicals are due to the spin leakage[27,34] from the phosphorus atom to the spin bearing nitrogen atom of phosphaverdazyl radical center. Here, the effective spin transmission is clearly represented from the strong spin density alternation pattern (Figure 5.2), as obvious from the MO analysis. For each species, a qualitative relation between SOMO–SOMO energy gaps with J values has been made. The shapes of SOMOs also play a

function to predict the state of magnetism (Figure 5.3). One also observes that the variation of average dihedral angles of the radical centers with the coupler plane determines the magnitude of J values. The kinetic stability as well as low chemical reactivity of Set-a diradicals than those of Set-b diradicals has been discussed in light of HOMO–LUMO energy gap. Finally, the ground state stability of these diradicals has also been investigated.

This work has been published in The Journal of Physical Chemistry A (Ref. 83).

5.5. References and Notes

(1) Kekulé, A. *Bull. Soc. Chim. Fr.* **1865**, *3*, 98.

(2) Erlenmeyer, E. *Ann. Chem. Pharm.* **1866**, *137*, 327.

(3) Pauling, L. *The Nature of the Chemical Bond and Structure of Molecules in Crystals*, Cornell University Press: Ithaca, pp 188ff, 1960.

(4) Cyrański, M. K.; Krygowski, T. M.; Katritzky, A. R.; Schleyer, P. v. R. *J. Org. Chem.* **2002**, *67*, 1333.

(5) Bird, C. W. *Tetrahedron* **1985**, *41*, 1409.

(6) Flygare, W. H. *Chem. Rev.* **1974**, *74*, 653.

(7) Breslow, R. *Angew. Chem. Int. Ed. Engl.* **1968**, *80*, 573.

(8) Krygowski, T. M.; Zachara, J. E.; Szatylwicz, H. *J. Org. Chem.* **2004**, *69*, 7038.

(9) Krygowski, T. M.; Cyrański, M. K. *Chem. Rev.* **2001**, *101*, 1385.

(10) Krygowski, T. M.; Cyrański, M. K. *Phys. Chem. Chem. Phys.* **2004**, *6*, 249.

(11) Chen, Z.; Wannere, C. S.; Corminboeuf, C.; Puchta, R.; Schleyer, P. v. R. *Chem. Rev.* **2005**, *105*, 3842.

(12) Schleyer, P. v. R.; Manoharan, M.; Jiao, H.; Stahl, F. *Org. Lett.* **2001**, *3*, 3643.

(13) Schleyer, P. v. R.; Maerker, C.; Dransfeld, A.; Jiao, H.; Hommes, N. J. R. v. E. *J. Am. Chem. Soc.* **1996**, *118*, 6317.

(14) Kahn, O. *Molecular Magnetism*, New York, VCH, 1993.

(15) Coronado, E.; Delhaè, P.; Gatteschi, D.; Miller, J. S. *Molecular Magnetism: From Molecular Assemblies to the Devices*, Eds.; Nato ASI Series E, Applied Sciences, Kluwer Academic Publisher: Dordrecht, Netherland, **1996**; Vol. 321.

(16) Hicks, R. G.; Ohrstrom, L.; Patenaude, G. W. *Inorg. Chem.* **2001**, *40*, 1865.

(17) Tamura, M.; Nakazawa, Y.; Shiomi, D.; Nozawa, K.; Hosokoshi, Y.; Ishikawa, M.; Takahashi, M.; Kinoshita, M. *Chem. Phys. Lett.* **1991**, *186*, 401.

(18) Ziessel, R.; Stroh, C.; Heise, H.; Khler, F. H.; Turek, P.; Claiser, N.; Souhassou, M.; Lecomte, C. *J. Am. Chem. Soc.* **2004**, *126*, 12604.

(19) Ali, Md. E.; Datta, S. N. *J. Phys. Chem. A* **2006**, *110*, 2776.

(20) Ali, Md. E.; Datta, S. N. *J. Phys. Chem. A* **2006**, *110*, 13232.

(21) Kuhn, R.; Trischmann, H. *Angew. Chem. Int. Ed. Engl.* **1963**, *2*, 155.

(22) Nesterenko, A. M.; Polumbrik, O. M.; Markovskii, L. M. *J. Struct. Chem.* **1984**, *25*, 209.

(23) Neugebauer, F. A.; Fischer, H.; Siegel, R. *Chem. Ber.* **1988**, *121*, 815.

(24) Koivisto, B. D.; Ichimura, A. S.; McDonald, R.; Lemaire, M. T.; Thompson, L. K.; Hicks, R. G. *J. Am. Chem. Soc.* **2006**, *128*, 690.

(25) Barclay, T. M.; Hicks, R. G.; Ichimura, A. S.; Patenaude, G. W. *Can. J. Chem.* **2002**, *80*, 1501.

(26) Azuma, N. *Bull. Chem. Soc. Jpn.* **1982**, *55*, 1357.

(27) Takeda, K.; Hamano, T.; Kawae, T.; Hidaka, M.; Takahashi, M.; Kawasaki, S.; Mukai, K. *J. Phys. Soc. Jpn.* **1995**, *64*, 2343.

(28) Mukai, K.; Konishi, K.; Nedachi, K.; Takeda, K. *J. Phys. Chem.* **1996**, *100*, 9658.

(29) Brook, D. J. R.; Fox, H. H.; Lynch, V.; Fox, M. A. *J. Phys. Chem.* **1996**, *100*, 2066.

(30) Serwinski, P. R.; Esat, B.; Lahti, P. M.; Liao, Y.; Walton, R.; Lan, J. *J. Org. Chem.* **2004**, *69*, 5247.

(31) Hicks, R. G.; Hooper, R. *Inorg. Chem.* **1999**, *38*, 284.

(32) Koivisto, B. D.; Hicks, R. G. *Coord. Chem. Rev.* **2005**, *249*, 2612.

(33) Bhattacharya, D.; Shil, S.; Misra, A.; Klein, D. J. *Theor. Chem. Acc.* **2009**, *127*, 57.

(34) Katritzky, A. R.; Belyakov, S. A.; Durst, H. D.; Xu, R.; Dalal, N. S. *Can. J. Chem.* **1994**, *72*, 1849.

(35) Kopf, P.; Morokuma, K.; Kreilick, R. *J. Chem. Phys.* **1971**, *54*, 105.

(36) Azuma, N.; Ishizu, K.; Mukai, K. *J. Chem. Phys.* **1974**, *61*, 2294.

(37) Fico, R. M., Jr.; Hay, M. F.; Reese, S.; Hammond, S.; Lambert, E.; Fox, M. A.; *J. Org. Chem.* **1999**, *64*, 9386.

(38) Krygowski, T. M. *J. Chem. Inf. Comput. Sci.* **1993**, *33*, 70.

(39) Kruszewski, J.; Krygowski, T. M. *Bull. Acad. Pol. Sci. Ser. Sci. Chim.* **1972**, *20*, 907.

(40) Lee, C. T.; Yang, W. T.; Parr, R. G. *Phys. Rev. B* **1988**, *37*, 785.

(41) Becke, A. D. *J. Chem. Phys.* **1993**, *98*, 5648.

(42) Hehre, W. J.; Ditchfield, R.; Pople, J. A. *J. Chem. Phys.* **1972**, *56*, 2257.

(43) Hariharan, P. C.; Pople, J. A. *Theor. Chim. Acta.* **1973**, *28*, 213.

(44) Francl, M. M.; Pietro, W. J.; Hehre, W. J.; Binkley, J. S.; Gordon, M. S.; Defrees, D. J.; Pople, J. A. *J. Chem. Phys.* **1982**, *77*, 3654.

(45) Noodleman, L. *J. Chem. Phys.* **1981**, *74*, 5737.

(46) Noodleman, L.; Baerends, E. J. *J. Am. Chem. Soc.* **1984**, *106*, 2316.

(47) Ginsberg, A. P. *J. Am. Chem. Soc.* **1980**, *102*, 111.

(48) Noodleman, L.; Davidson, E. R. *Chem. Phys.* **1986**, *109*, 131.

(49) Noodleman, L.; Peng, C. Y.; Case, D. A.; Mouesca, J. -M. *Coord. Chem. Rev.* **1995**, *144*, 199.

(50) Bencini, A.; Totti, F.; Daul, C. A.; Doclo, K.; Fantucci, P.; Barone, V. *Inorg. Chem.* **1997**, *36*, 5022.

(51) Bencini, A.; Gatteschi, D.; Totti, F.; Sanz, D. N.; McClevrty, J. A.; Ward, M. D. *J. Phys. Chem. A* **1998**, *102*, 10545.

(52) Ruiz, E.; Cano, J.; Alvarez, S.; Alemany, P. *J. Comput. Chem.* **1999**, *20*, 1391.

(53) Martin, R. L.; Illas, F. *Phys. Rev. Lett.* **1997**, *79*, 1539.

(54) Caballol, R.; Castell, O.; Illas, F.; de Moreira, I. P. R.; Malrieu, J. P. *J. Phys. Chem. A* **1997**, *101*, 7860.

(55) Barone, V.; di Matteo, A.; Mele, F.; de Moreira, I. P. R.; Illas, F. *Chem. Phys. Lett.* **1999**, *302*, 240.

(56) Illas, F.; de Moreira, I. P. R.; de Graaf, C.; Barone, V. *Theor. Chem. Acc.* **2000**, *104*, 265.

(57) de Graaf, C.; Sousa, C.; de Moreira, I. P. R.; Illas, F. *J. Phys. Chem. A* **2001**, *105*, 11371.

(58) Illas, F.; de Moreira, I. P. R.; Bofill, J. M.; Filatov, M. *Phys. Rev. B* **2004**, *70*, 132414.

(59) Ciofini, I.; Daul, C. A. *Coord. Chem. Rev.* **2003**, *238*, 187.

(60) Yamaguchi, K.; Takahara, Y.; Fueno, T.; Nasu, K. *Jpn. J. Appl. Phys.* **1987**, *26*, L1362.

(61) Yamaguchi, K.; Jensen, F.; Dorigo, A.; Houk, K. N. *Chem. Phys. Lett.* **1988**, *149*, 537.

(62) Yamaguchi, K.; Takahara, Y.; Fueno, T.; Houk, K. N. *Theor. Chim. Acta.* **1988**, *73*, 337.

(63) Latif, I. A.; Panda, A.; Datta, S. N. *J. Phys. Chem. A* **2009**, *113*, 1595.

(64) Bhattacharya, D.; Misra, A. *J. Phys. Chem.* A **2009**, *113*, 5470.

(65) Gräfenstein, J.; Kraka, E.; Filatov, M.; Cremer, D. *Int. J. Mol. Sci.* **2002**, *3*, 360.

(66) Ruiz, E.; Alvarez, S.; Cano, J.; Polo, V. *J. Chem. Phys.* **2005**, *123*, 164110.

(67) Frisch, M. J.; Trucks, G. W.; Schlegel, H. B.; Scuseria, G. E.; Robb, M. A.; Cheeseman, J. R.; Montgomery, J. A. Jr.; Vreven, T.; Kudin, K. N.; Burant, J. C.; Millam, J. M.; Iyengar, S. S.; Tomasi, J. J.; Barone, V.; Mennucci, B.; Cossi, M.; Scalmani, G.; Rega, N.; Petersson, G. A.; Nakatsuji, H.; Hada, M.; Ehara, M.; Toyota, K.; Fukuda, R.; Hasegawa, J ; Ishida, M.; Nakajima, T.; Honda, Y.; Kitao, O.; Nakai, H.; Klene, M.; Li, X.; Knox, J. E.; Hratchian, H. P.; Cross, J. B.; Bakken, V.; Adamo, C.; Jaramillo, J.; Gomperts, R.; Stratmann, R. E.; Yazyev, O.; Austin, A J.; Cammi, R.; Pomelli, C.; Ochterski, J.; Ayala, P. Y.; Morokuma, K.; Voth, A.; Salvador, P.; Dannenberg, J. J.; Zakrzewski, V. G.; Dapprich, S.; Daniels, A. D.; Strain, M. C.; Farkas, O.; Malick, D. K.; Rabuck, A. D.; Raghavachari, K.; Foresman, J. B.; Ortiz, J. V.; Cui, Q.; Baboul, A. G.; Clifford. S.; Cioslowski, J.; Stefanov, B. B.; Liu, G.; Liashenko, A.; Piskorz, P.; Komaromi, I.; Martin, R. L.; Fox, D. J.; Keith, T.; Al-Laham, M. A.; Peng, C. Y.; Nanayakkara, A.; Challacombe, M.; Gill, P. M. W.; Johnson, B.; Chen, W.; Wong, M. W.; Gonzalez, C.; Pople, J. A. GAUSSIAN 03W (Revision D.01), Gaussian, Inc.:Wallingford, CT, (2004). Gaussian Inc., Wallingford, CT.

(68) Hyperchem Professional Release 7.5 for Windows, Hypercube Inc.: Gainesville, FL, 2002.

(69) Flükiger, P.; Lüthi, H. P.; Portmann, S.; Weber, J. MOLEKEL 4.0, J. Swiss Center for Scientific Computing, Manno, Switzerland, 2000.

(70) Hoppe, U.; Walter, G.; Barz, A.; Stachel, D.; Hannon, A. C. *J. Phys. Cond. Mat.* **1998**, *10*, 261.

(71) Markovski, L. N.; Romanenko, V. D.; Ruban, A. V. *Pure. Appl. Chem.* **1987**, *59*, 1047.

(72) Trindle, C.; Datta, S. N. *Int. J. Quantum Chem.* **1996**, *57*, 781.

(73) Trindle, C.; Datta, S. N.; Mallik, B. *J. Am. Chem. Soc.* **1997**, *119*, 12947.

(74) Polo, V.; Alberola, A.; Andres, J.; Anthony, J.; Pilkington, M. *Phys. Chem. Chem. Phys.* **2008**, *10*, 857.

(75) Hoffmann, R.; Zeiss, G. D.; Van Dine, G. W. *J. Am. Chem. Soc.* **1968**, *90*, 1485.

(76) Constantinides, C. P.; Koutentis, P. A.; Schatz, J. *J. Am. Chem. Soc.* **2004**, *126*, 16232.

(77) Zhang, G.; Li, S.; Jiang, Y. *J. Phys. Chem. A* **2003**, 107, 5573.

(78) Hay, P. J.; Thibeault, C. J.; Hoffmann, R. *J. Am. Chem. Soc.* **1975**, *97*, 4884.

(79) Fukai, K.; Yonezawa, T.; Shingu, H. *J. Am. Chem. Soc.* **1952**, *93*, 2413.

(80) Aihara, J. *J. Phys. Chem. A* **1999**, *103*, 7487.

(81) Zhou, Z.; Parr, R. G. *J. Am. Chem. Soc.* **1990**, *112*, 5720.

(82) Salcedo, R. *J. Mol. Model.* **2007**, *13*, 1027.

(83) Bhattacharya, D.; Shil, S.; Panda, A.; Misra, A. *J. Phys. Chem. A.* **2010**, *114*, 11833.